Dense bubble flow in a silo: An unusual flow of a dispersed medium

Yann Bertho, Christophe Becco, and Nicolas Vandewalle
Group for Research and Applications in Statistical Physics (GRASP), Institut de Physique B5a, Université de Liège, 4000 Liège, Belgium

(Received 12 August 2005; published 23 May 2006)

The dense flow of air bubbles in a two-dimensional silo (through an aperture D) filled with a liquid is studied experimentally. A particle tracking technique has been used to bring out the main properties of the flow: displacements of the bubbles, transverse, and axial velocities. The behavior of the air bubbles is observed to present similarities with nondeformable solid grains in a granular flow. Nevertheless, a correlation between the bubble velocities and their deformations has been evidenced. Moreover, a new discharge law (Beverloo like) must be considered for such a system, where the flow rate is observed to vary as $D^{1/2}$ and depends on the deformability of the particles.

DOI: 10.1103/PhysRevE.73.056309 PACS number(s): 47.60.+i, 47.50.−d, 82.70.−y, 83.50.−v

Structured fluids like granular materials or aqueous foams received much attention from physicists during the last decade. Indeed, they are ubiquitous in nature and in industrial processes [1,2], and exhibit striking rheological behaviors as compared to conventional liquids. These materials involve multiple physical processes and cooperative phenomena such as shear banding, particle interactions, and the formation of arches redirecting the forces inside the material [3,4]. Such processes are then able to provoke intermittent flows [5] or jamming [6] because of the topological constraints that develop since the particles (grains or bubbles) press against each other. This contributes to the complex flow behavior of granular media and foams.

The present study deals with bubble assemblies where the bubbles are predominantly oblate so that the contacts between two adjacent bubbles are reduced [see Fig. 1(b)]. The liquid fraction in the material is high enough to consider the diffusion of air through the bubble boundaries as negligible at the time scale of the experiments.

Bubble assemblies can also be seen as a granular medium where contacting particles are characterized by a nearly zero friction. Thus, we have a remarkable system with a low-energy dissipation at the contacts in comparison with traditional grain assemblies. Both granular media and foams are model systems for divided materials. Nevertheless, even if bubble flows present qualitative analogies with granular flows, we must keep in mind that the nature of the interactions between the particles is totally different. Moreover, in contrast with granular materials, the bubbles may undergo strong deformations when they are subjected to a constraint. Many works deal with the study of flowing foams (velocity profiles, bubble deformations) in a Couette geometry [7,8] or through a constriction [9]. In contrast with this latter paper dealing with a dry foam flowing in a Hele-Shaw cell, our interest concerns wet foams flowing between a plate and the liquid surface. Instantaneous measurements of velocity and deformation of the bubbles are reported. The dependence of the bubble flow rate regarding the aperture or the mean bubble velocity is analyzed through the comparison with granular materials in the same geometry.

In this paper, the flow of a two-dimensional (2D) foam is analyzed experimentally [10,11]. The setup consists of a transparent inclined glass plane of width $W=130$ mm which is immersed into water [Fig. 1(a)]. The tilt angle θ of the plane can be adjusted by a fine screwing system. Quasi monodisperse air bubbles are then injected at the bottom of the inclined plane by blowing air through a needle (the height h of the piling is kept roughly constant during the experiments $h \simeq 200$ mm). Note that the tilt angle is small (θ ranges from 0° to 1°) to ensure that only one layer of bubbles is created in the perpendicular direction to the plane and to decrease the influence of the gravity (i.e., liquid drainage). Bubble size is controlled by an air pump and is kept roughly constant in the present study [diameter $d=(5.4\pm0.3)$ mm]. In order to avoid the coalescence of the bubbles, dish-washing liquid based on anionic surfactant AEOS-2EO is mixed into water [12]. The surface tension of the solution is $\gamma \simeq 25$ mN m^{-1}, leading to a capillary length $\kappa^{-1}=\sqrt{\gamma/(\rho g)} \simeq 1.6$ mm. In our experiment, the bubbles are larger than κ^{-1} and consequently adopt an oblate shape [Fig. 1(b)] so that the contact between two adjacent bubbles is reduced. Due to buoyancy, the bubbles rise underneath the inclined plane and tend to pack on a transverse wall placed at the top of the plane. An orifice of width D at the center (x_0, y_0) of this obstacle allows the bubbles to empty out the silo. Our experiment is then analogous to the gravity-driven granular flow in a flat bottomed 2D silo, emptying out of a central orifice [13]. Top views of the bubble packing are recorded through the transparent tilted plane by means of a charge-coupled-device (CCD) camera at a frame rate of 50 frames per second. In order to quantify and to measure the main properties of the flow, the motion of each bubble (≈2000 bubbles per frame) has been tracked through image analysis.

Figure 2 displays typical transverse v_x and longitudinal v_y velocities of the bubbles as a function of x and y at different heights in the packing. In the top part of the silo [(△) in Fig. 2(b)], a block motion is observed: the longitudinal velocity v_y remains constant reflecting low interactions between the bubbles and the side walls (slipping motion). As y decreases (i.e., the bubbles move towards the outlet), the flow takes place in a triangular-shaped domain where the fastest bubbles are located in the center of the silo and the slowest or motionless ones at the walls [(▼) in Fig. 2(b)]. This is in agreement with the V shape of mobile grains observed during the flow of granular materials in silos or hourglasses [14,13]. Far from the outlet ($y \gtrsim 15d$), bubbles have a nearly

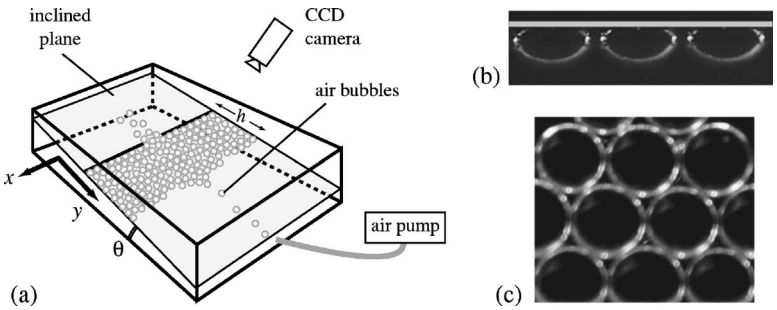

FIG. 1. (a) Sketch of the experimental setup. A transparent inclined plane is immersed into water and tilted at an angle θ. Small air bubbles are injected from below at the bottom of the plane and rise towards the top where they aggregate. Motions of the bubbles are recorded by a CCD camera. (b) Side view: the bubbles present an oblate shape. (c) Top view: the bubbles have a circular shape in the bulk.

zero transverse velocity [Fig. 2(c)] and a constant longitudinal velocity v_y [Fig. 2(d)]. For lower values of y, the velocity distribution of the bubbles deep inside the silo is totally modified: a transverse component of velocity v_x appears in the flow conducting the bubbles towards the orifice while v_y increases strongly near the outlet.

A close-up of the bottom part of the silo of height 60 mm is shown in Fig. 3(a). Image analysis allows one to extract the position of each bubble in the stack and evaluate the displacement profile [Fig. 3(b)] and the velocity field [Fig. 3(c)] during the flow. Figure 3(d) displays the deformation field and provides information concerning the constraints undergone inside the dense bubble assembly. In contrast with granular materials where the flow occurs only in a cone-shaped central region of the silo (while the grains located in the regions near the side walls are motionless) [14,13], note that motions of bubbles are detected everywhere in the silo. Moreover, the bubble tracking put into evidence recirculation zones and the propagation of dislocations (shear bands) during the bubble flow. As expected in two-dimensional nearly monodisperse flows, bubbles tend to pack in an ordered hexagonal structure at the top of the bubble packing [Fig. 3(a)]; these organized domains are separated by the dislocations. Motions of blocks of bubbles are observed and look like crystal domains. Those blocks are sliced by fast-moving defects along bubble lines. The movement is not simultaneous along the whole row but begins at one end with the appearance of a dislocation running along the slip line. This process is initiated at the orifice of the silo and propagates towards the bulk after many rebounds on the side walls. Both recir-

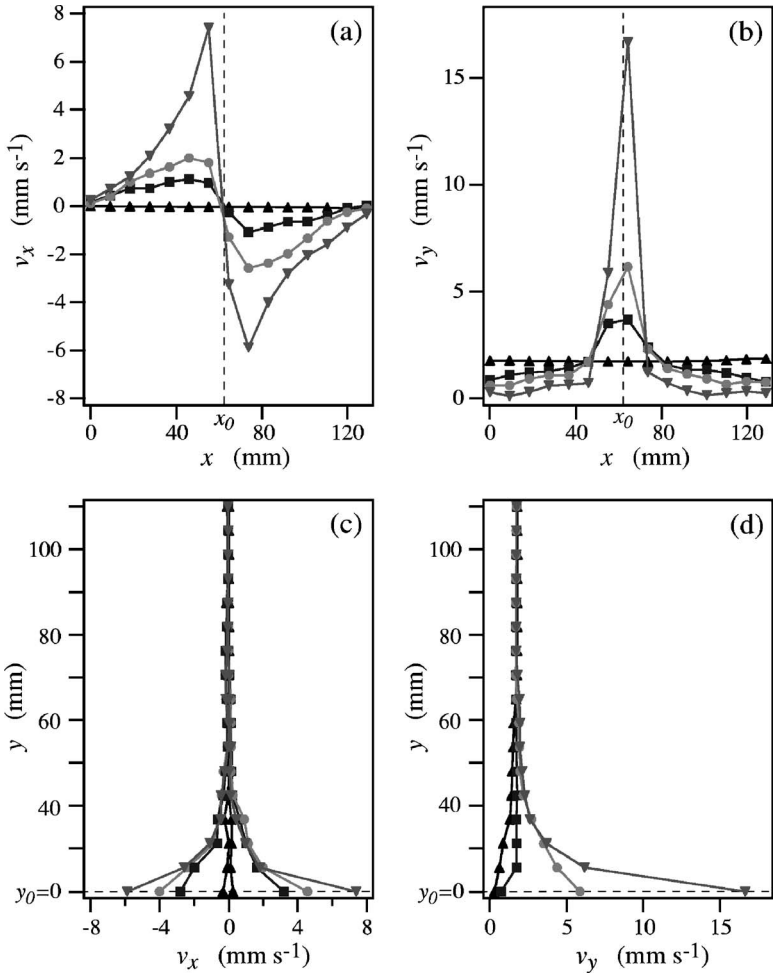

FIG. 2. Transverse v_x and longitudinal v_y velocity profiles during the discharge of a silo ($\theta \simeq 0.63°$, $D \simeq 8.6$ mm). Dashed line: position (x_0, y_0) of the center of the outlet of the silo. The different curves (▼, ●, ■, ▲) correspond, respectively, to velocity profiles at increasing distances from $y_0=0$ and increasing distances from x_0.

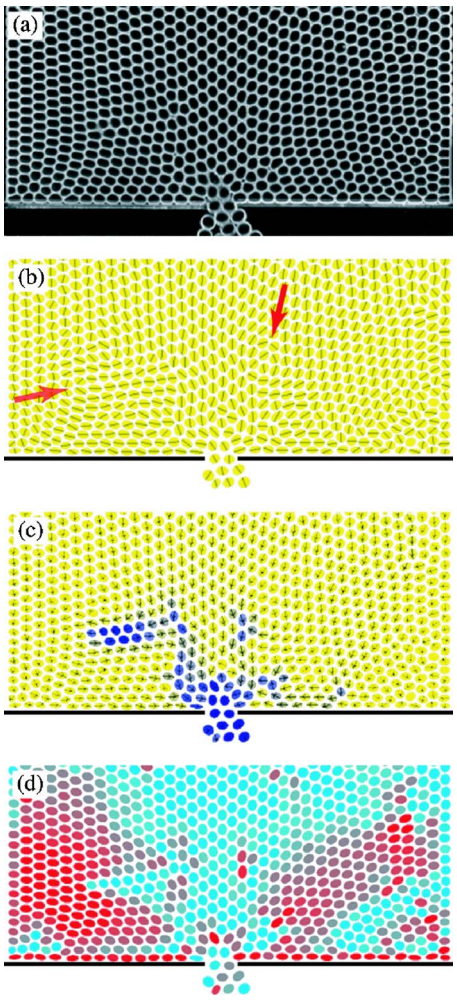

FIG. 3. (Color online) Typical recordings of the bubble discharge: (a) Snapshot of the experimental flow. (b) Displacement field. The arrows point out a dislocation and a recirculation zone. (c) Velocity field. The fastest bubbles appear in blue (or darker). (d) Deformation field. The more constrained bubbles appear in red (or darker) while circular bubbles appear in blue.

culation zone and dislocation appear clearly as pointed out by the arrows in Fig. 3(b).

The instantaneous velocity $v=(v_x^2+v_y^2)^{1/2}$ of each bubble has been computed and superimposed on the images of the flow (the darkest—or blue—bubbles corresponding to the fastest ones). The recirculation regions and the dislocation observed in Fig. 3(b) are characterized by a mean velocity higher than in the rest of the silo [Fig. 3(c)].

The deformation of a bubble is evaluated by fitting the bubble shape by an ellipse and computing its eccentricity [15]. As pointed out in Fig. 3(d), the fastest bubbles are observed to correspond to the less deformed ones. Moving bubbles press against surrounding ones and deform them. This is especially the case near the dislocation. Therefore, in such dense bubble flows, spherical bubbles are located far from the outlet and propagate in a block motion at a constant velocity or in the dislocation, while flattest ones correspond to crushed bubbles against the bottom wall or constraint bubbles inside the pile.

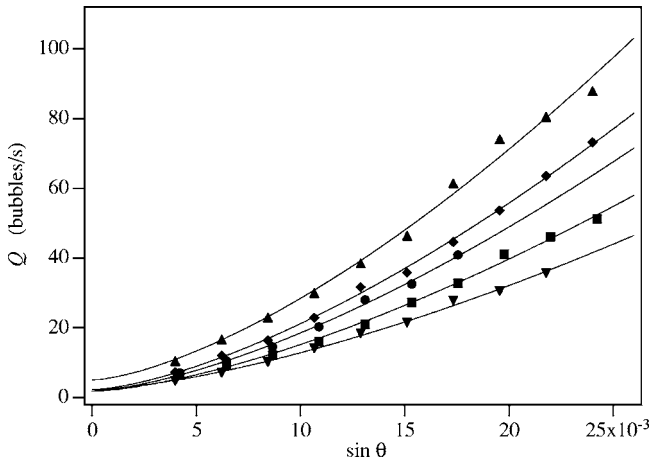

FIG. 4. Bubble flow rate Q as a function of the tilt angle θ of the plane. The curves correspond to different apertures D of the silo: (▼) $D=6.3$ mm, (■) $D=8.0$ mm, (●) $D=9.7$ mm, (♦) $D=12.8$ mm, and (▲) $D=19.9$ mm. Solid line: best fit of the experimental data with $Q\propto(\sin\theta)^{3/2}$.

A classic paper on the flow of particles through orifices is that of Beverloo *et al.* [16]. Using a straightforward dimensional analysis, they pointed out that the grain flow rate Q_g is a power law in D (where D is the diameter of the orifice). The power depends on the dimensionality of the flow [14,16,17], so that for a 2D flow $Q_g\propto g^{1/2}D^{3/2}$. A corrective term is usually added to take into account the mean diameter of the grains d_g:

$$Q_g \propto g^{1/2}(D-kd_g)^{3/2}, \tag{1}$$

where k is an empirical constant depending on the particle shape and the grain interactions ($k\simeq 1.5$ for beads). This law characterizing the dynamical properties of the grain flow does not invoke explicitly dissipative mechanisms. However, we expect that k and the value of the exponent 3/2 contain implicitly friction and deformation of the grains even if the dependence of these parameters with friction and deformability is still an open question.

The bubble flow rate Q has been evaluated by counting the number of bubbles flowing out of the silo, at different tilt angles θ of the plane. Figure 4 shows that Q varies as $(\sin\theta)^{3/2}$, where the tilt angle plays a similar part to gravity encountered in the traditional Beverloo's law. The behavior of bubble flow through an aperture is thus drastically different from the one of a granular flow for which Q_g varies as $g^{1/2}$. This is probably due to the nature of forces between the particles and with the walls: the frictions inside a granular medium are much more important than in a bubble flow and consequently slow down the silo discharge.

Figure 5 displays the bubble flow rate Q as a function of the normalized aperture of the silo D/d. In contrast with granular materials for which the flow rate Q_g vanishes for $D/d\lesssim 1.5$ due to the formation of arches [Eq. (1)], Q is observed to be nonzero for smaller values of the aperture. Bubbles can pass through an orifice of the order of $2d/3$ after having undergone strong shape deformations. The value of $k\simeq 2/3$ should then depend mainly on the bubble size and

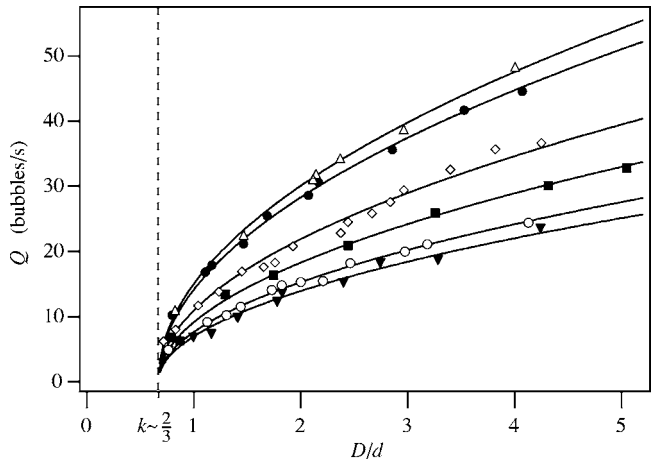

FIG. 5. Bubble flow rate Q as a function of the aperture D of the silo (normalized by the mean bead diameter d). The curves correspond to different tilt angles θ of the plane: (▼) θ=0.46°, (○) θ=0.50°, (■) θ=0.56°, (◇) θ=0.63°, (●) θ=0.75°, and (△) θ=0.82°. Solid line: best fit of the experimental data with $Q \propto (D/d-k)^{1/2}$; k presents very low dispersion and verifies $k=(0.66\pm0.03)\simeq\frac{2}{3}$.

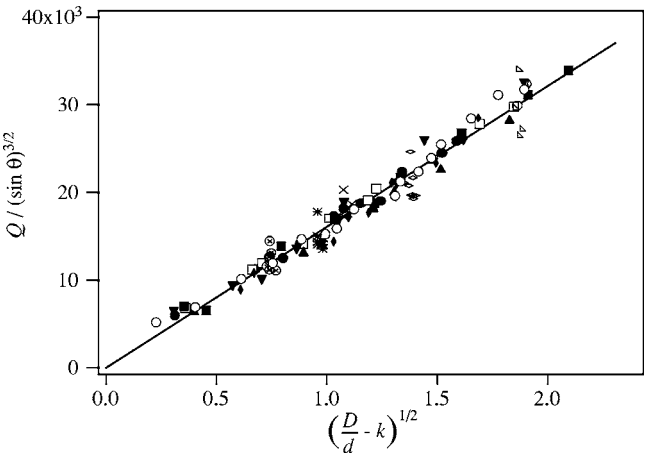

FIG. 6. Rescaling of all measurements using Eq. (3) for the data presented in Figs. 4 and 5.

the surface tension of the liquid; these assumptions will receive special care in a subsequent work. Moreover, note that Q varies as $(D/d)^{1/2}$ which is significantly different from the case of a nondeformable 2D granular material flowing down a silo where the power is 3/2.

The bubbles at the outlet of the silo are affected by the buoyancy B coming from the bubbles located behind them. This buoyancy presents a nontrivial law because it does not result directly from the sum of each individual bubble in the stack: a part of the energy is dissipated through the deformation of the bubbles. Let us assume that the driving force is the buoyancy component along the plane, so that $B \propto g \sin\theta$.

The dissipation relationship linking the drag force f to a given velocity v is nontrivial and known to involve rather subtle hydrodynamics [18,19]. If Archimedes' forces were balanced by a Stokes' viscous force ($f \propto \eta d v$), this would provide a constant rise velocity proportional to $\sin\theta$. But for a single bubble creeping along a slightly inclined plane immersed in a viscous fluid, it has been shown that the creeping velocity v does not vary linearly with the tilt angle $\sin\theta$ [20]. Moreover, the viscous dissipation is known to be sensitive to the surface mobility of the surfactant [19]. For our surfactant which leads to tangentially mobile bubble surfaces, if we consider the viscous dissipation associated with the formation of a lubricating film between the single bubble and the plane, the viscous force f is observed to vary as $\gamma^{1/12}(\eta v)^{2/3}$.

Assuming in a first approximation that the dynamics of the flow are mainly governed by these two forces (neglecting therefore the interactions between the bubbles), the equilibrium between the buoyancy and the drag force leads to a terminal velocity v proportional to $(\sin\theta)^{3/2}$. Therefore, the bubble flow rate $Q=vD/d^2$ can be written

$$Q \propto \frac{(g \sin\theta)^{3/2}}{\eta \gamma^{1/8}}, \tag{2}$$

which agrees with behaviors emphasized in Fig. 4. Moreover, as expected, the bubble flow rate is then observed to decrease when the viscosity η of the fluid is increased. This straightforward model reproduces the main effects observed experimentally and enhances the fact that a new Beverloo's law must be considered in the particular case of bubble flows and more generally the flow of deformable dispersed media.

Figure 6 displays a rescaling of all measurements and confirms that Beverloo's law for a deformable dispersed medium is given by

$$Q \propto (g \sin\theta)^{3/2}\left(\frac{D}{d}-k\right)^{1/2}, \tag{3}$$

where $k<1$ is related to the deformation ability of the particles and the friction between particles. More experiments must now be performed to distinguish the influence of both friction and deformation on k and on the value of the exponent. Numerical simulations are currently performed on this topic and will be the object of a subsequent publication. Finally, following the approach proposed by Asipauskas *et al.* [9], the study of the influence of the bubble deformation on the flux measured at the outlet of the silo would provide a good complement to the present study.

In summary, the present experiment shows that the velocity profiles for bubble flows in silos present qualitative similarities with a granular flow but with sliding motions at the walls. A correlation between the velocity and the deformation of the bubbles has been observed. Moreover, we demonstrate that a new Beverloo's law must be considered for the specific case of deformable dispersed media flowing out a silo, where the flow rate varies as $D^{1/2}$ and depends on the nature of the interactions between particles and their capability to deform themselves when they are submitted to a constraint.

The authors thank G. Broze and S. Dorbolo for helpful discussions during this work. Y.B. is supported by ARC Program No. 02/07-293 and ESA MAP "AO-99-108."

[1] J. Duran, *Sands, Powders and Grains* (Springer-Verlag, 2000).
[2] D. Weaire and S. Hutzler, *The Physics of Foams* (Oxford University Press, Oxford, 1999).
[3] H. A. Janssen, Versuche über Getreidedruck in Silozellen, Z. Ver. Dtsch. Ing. **39**, 1045 (1895).
[4] Y. Bertho, F. Giorgiutti-Dauphiné, and J. P. Hulin, Phys. Rev. Lett. **90**, 144301 (2003).
[5] Y. Bertho, F. Giorgiutti-Dauphiné, and J. P. Hulin, Phys. Fluids **15**, 3358 (2003).
[6] S. Rodts, J. C. Baudez, and P. Coussot, Europhys. Lett. **69**, 636 (2005).
[7] J. Lauridsen, G. Chanan, and M. Dennin, Phys. Rev. Lett. **93**, 018303 (2004).
[8] E. Janiaud and F. Graner, J. Fluid Mech. **532**, 243 (2005).
[9] M. Asipauskas, M. Aubouy, J. A. Glazier, F. Graner, and Y. Jiang, Granular Matter **5**, 71 (2003).
[10] W. L. Bragg and J. F. Nye, Proc. R. Soc. London, Ser. A **190**, 474 (1947).
[11] N. Vandewalle, S. Trabelsi, and H. Caps, Europhys. Lett. **65**, 316 (2004).
[12] Alkyl ether sulfate—2 ethylene oxide (leading to mobile bubble surfaces), fully described in G. Broze, *Handbook of Detergents*, Surfactant Science Series (Marcel Dekker, New York, 1999).
[13] A. Medina, J. Andrade, and C. Trevino, Phys. Lett. A **249**, 63 (1998).
[14] D. Hirshfeld, Y. Radzyner, and D. C. Rapaport, Phys. Rev. E **56**, 4404 (1997).
[15] C. Ybert and J.-M. di Meglio, C. R. Phys. **3**, 555 (2002).
[16] W. A. Beverloo, H. A. Leniger, and J. V. D. Velde, Chem. Eng. Sci. **15**, 260 (1961).
[17] A. A. Mills, S. Day, and S. Parkes, Eur. J. Phys. **17**, 97 (1996).
[18] F. P. Bretherton, J. Fluid Mech. **10**, 166 (1961).
[19] N. D. Denkov, V. Subramanian, D. Gurovich, and A. Lips, Colloids Surf., A **263**, 129 (2005).
[20] P. Aussillous and D. Quéré, Europhys. Lett. **59**, 370 (2002).